

Learning Domain Knowledge in Multimodal Large Language Models through Reinforcement Fine-Tuning

Qinglong Cao^{1,2} Yuntian Chen² Chao Ma¹ Xiaokang Yang¹

Abstract

Multimodal large language models (MLLMs) have shown remarkable capabilities in multimodal perception and understanding tasks. However, their effectiveness in specialized domains, such as remote sensing and medical imaging, remains limited. A natural approach to domain adaptation is to inject domain knowledge through textual instructions, prompts, or auxiliary captions. Surprisingly, we find that such input-level domain knowledge injection yields little to no improvement on scientific multimodal tasks, even when the domain knowledge is explicitly provided. This observation suggests that current MLLMs fail to internalize domain-specific priors through language alone, and that domain knowledge must be integrated at the optimization level. Motivated by this insight, we propose a reinforcement fine-tuning framework that incorporates domain knowledge directly into the learning objective. Instead of treating domain knowledge as descriptive information, we encode it as domain-informed constraints and reward signals, shaping the model’s behavior in the output space. Extensive experiments across multiple datasets in remote sensing and medical domains consistently demonstrate good performance gains, achieving state-of-the-art results on multimodal domain tasks. Our results highlight the necessity of optimization-level domain knowledge integration and reveal a fundamental limitation of textual domain conditioning in current MLLMs.

1. Introduction

Multimodal large language models (MLLMs) have demonstrated strong generalization abilities across a wide range of

¹MoE Key Lab of Artificial Intelligence, AI Institute, Shanghai Jiao Tong University, Shanghai, China ²Eastern Institute of Technology, Ningbo, China. Correspondence to: Yuntian Chen <ychen@eitech.edu.cn>.

Preprint. January 26, 2026.

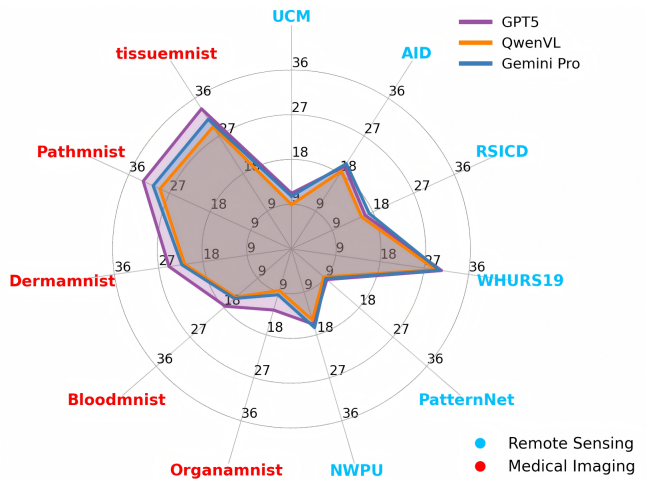


Figure 1. Performance comparison in specialized domains with multimodal large language models.

	UCM	AID	RSICD	WHURS19	PatternNet	NWPU
QwenVL	8.91	18.6	15.5	29.3	8.62	14.9
+ Domain Prompt	8.89	18.5	15.4	29.1	8.71	14.9
+ Caption(MLLM)	6.42	15.8	15.3	26.1	5.23	10.5
+ Caption(BLIP)	8.62	18.1	15.2	28.8	8.52	14.7
Ours	28.8	38.9	26.4	44.4	19.1	36.4

Table 1. Performance comparison by injecting domain knowledge with different fine-tuning methods.

vision-language tasks (Achiam et al., 2023; Bai et al., 2025; Lu et al., 2025; Xu et al., 2025; Cao et al., 2025), leading to remarkable progress in diverse application domains (Jiang et al., 2025a; Wang et al., 2025b; Sun et al., 2025; Jiang et al., 2025b). Despite these successes, their effectiveness in specialized scientific domains remains limited. As illustrated in Figure 1, advanced MLLMs typically achieve only 20%–30% accuracy on benchmarks from remote sensing and medical imaging, indicating substantial challenges in cross-domain generalization.

A natural strategy to address this limitation is to explicitly inject domain knowledge into MLLMs through prompts or auxiliary textual descriptions. Thus, we systematically investigate such approaches in the remote sensing domain. Specifically, we explore (i) domain-aware prompting that

explicitly encodes domain properties (e.g., rotation invariance), and (ii) caption-based augmentation, where auxiliary captions are either generated by MLLMs themselves or provided by an external captioning model (BLIP (Li et al., 2023)). However, as shown in Table 1, these naive forms of domain knowledge injection do not consistently improve performance. In several cases, caption-based augmentation even degrades accuracy, suggesting that simply providing additional domain-related text is insufficient and may introduce misleading or noisy signals.

These observations suggest that current MLLMs are unable to directly internalize high-level domain knowledge through naive textual conditioning. A key challenge is that domain knowledge is often abstract and conceptual rather than instance-level, and therefore cannot be easily translated into large-scale supervised annotations. Moreover, for specialized domains, such annotations are typically expensive and difficult to acquire. As a result, conventional supervised fine-tuning (SFT) (Dong et al., 2024; Zhang et al., 2025b; Yuan et al., 2024), which relies heavily on explicit input–output pairs, is insufficient for effectively injecting domain knowledge into the model.

In contrast, reinforcement learning (Guo et al., 2025; Zhang et al., 2024; Wang et al., 2024b; Yue et al., 2025), which does not require dense supervision, provides a natural mechanism for incorporating abstract domain principles at the optimization level. By defining reward signals that reflect domain-specific constraints or desiderata, reinforcement learning enables models to gradually align their reasoning behaviors with domain knowledge, even in the absence of large-scale annotations.

Motivated by this insight, we propose a reinforcement fine-tuning framework that integrates domain knowledge directly into the learning objective, as shown in Table 1, enabling MLLMs to acquire domain-aware reasoning capabilities beyond what is achievable with prompt-based or supervised approaches. Specifically, we introduce a domain-aware constraint loss that explicitly encodes domain knowledge as optimization constraints. This constraint loss is incorporated into the reinforcement learning process, shaping the model’s policy toward domain-consistent reasoning behaviors. Rather than relying on explicit supervision, the proposed constraint guides the model to satisfy abstract domain principles during optimization.

In addition, we quantify the degree of domain relevance for each training sample and leverage this information to reweight the reinforcement learning advantages. By assigning higher advantages to samples that exhibit stronger domain-specific characteristics, the learning process emphasizes domain-aware trajectories and suppresses spurious or domain-agnostic behaviors. Together, the constraint loss and the advantage reweighting mechanism jointly constitute

a domain knowledge-aware reinforcement signal, enabling effective domain knowledge injection even under limited annotations.

Through this unified framework, domain knowledge is no longer treated as external conditioning, but is internalized as part of the model’s optimization objective, resulting in robust and generalizable domain-aware reasoning. We conduct extensive evaluations across diverse datasets in both remote sensing and medical imaging domains. The results consistently validate the effectiveness of the proposed framework, demonstrating its ability to induce domain-aware reasoning behaviors across heterogeneous multimodal tasks. In summary, we make the following contributions:

- To the best of our knowledge, we first proposed a reinforcement fine-tuning paradigm that explicitly injects domain knowledge into multimodal large language models at the optimization level, moving beyond prompt-based or supervised domain adaptation.
- We develop a domain-aware reinforcement learning framework that integrates domain knowledge directly into the learning objective through domain-specific constraints and reward shaping, together with a domain knowledge-aware advantage reweighting strategy that emphasizes domain-relevant samples during training.
- We demonstrate the effectiveness of the proposed framework through extensive experiments on remote sensing and medical imaging benchmarks, achieving state-of-the-art performance across a wide range of multimodal domain-specific tasks.

2. Related Work

Multimodal Large Language Models. Multimodal large language models (MLLMs), such as GPT-4V (Achiam et al., 2023) and Qwen-VL (Bai et al., 2025), have demonstrated remarkable capabilities in jointly understanding and reasoning over visual and textual inputs. Recent advances show that MLLMs can effectively serve as general-purpose multimodal agents, enabling a wide range of downstream tasks that require vision–language perception, interaction, and decision making (Li et al., 2024; Huang et al., 2024a; Han et al., 2024). These models have been successfully applied to diverse multimodal applications, including visual editing, multimodal reasoning, and interactive response generation (Huang et al., 2024b; Zang et al., 2025; Luo et al., 2025b; Wang et al., 2025a). From a training perspective, the development of MLLMs typically consists of two stages. The first stage is large-scale multimodal pre-training (Luo et al., 2025a; Lin et al., 2024; Fan et al., 2024), which leverages massive image–text data to endow the model with general multimodal representations and broad world knowledge. The second stage is post-training (Cheng et al., 2024; Wang

et al., 2024a; Cheng et al., 2025), which includes instruction tuning, reinforcement learning, and alignment techniques, aiming to improve instruction following, response quality, and reasoning behavior. While these post-training strategies have proven effective for general-purpose tasks, their ability to inject domain knowledge into MLLMs remains limited, especially in specialized scientific domains.

Reinforcement Learning for MLLMs. With the emergence of reasoning-oriented models such as OpenAI-o1 (Jaech et al., 2024) and DeepSeek-R1 (Liu et al., 2024; Guo et al., 2025), increasing attention has been devoted to leveraging reinforcement learning (RL) to enhance the reasoning capabilities of MLLMs. Reinforcement learning provides a flexible optimization framework that allows models to be trained with preference signals or task-level objectives, without relying on dense supervised annotations. Conventional RL-based alignment methods include Proximal Policy Optimization (PPO) (Schulman et al., 2017), which optimizes policies under a KL-regularized constraint, and Direct Preference Optimization (DPO) (Rafailov et al., 2023) which eliminates the need for an explicit reward model by directly learning from pairwise preferences. More recently, Group Relative Policy Optimization (GRPO) (Shao et al., 2024) has been proposed as an efficient alternative that estimates advantages using group-wise comparisons, significantly reducing computational overhead while maintaining stable training dynamics. Due to its favorable efficiency and scalability, GRPO has become a widely adopted reinforcement learning paradigm for training large language models (Zhang et al., 2025a;c; Ramesh et al., 2024; Gao et al., 2024). Particularly, Visual-RFT (Liu et al., 2025) adopts it for visual perception tasks. In this work, we adopt GRPO as the underlying reinforcement learning framework. By integrating domain-aware constraints and domain knowledge-guided reward shaping into the GRPO objective, our approach enables reinforcement learning to explicitly guide MLLMs toward domain-consistent reasoning behaviors.

3. Method

As illustrated in Figure 2, our goal is to adapt multimodal large language models (MLLMs) to specialized domains such as remote sensing and medical imaging. Unlike conventional supervised fine-tuning (SFT) or prompt-based domain injection, our approach internalizes domain knowledge through reinforcement fine-tuning. We focus on abstract and structural domain knowledge that cannot be easily expressed via textual supervision, such as rotation invariance in remote sensing and symmetry consistency in medical imaging. To incorporate such knowledge, we adopt GRPO as the base reinforcement learning framework, enabling domain knowledge to be integrated directly at the policy optimization level. Our method consists of two key components. First, we con-

struct a *domain-support sampling distribution* that explicitly encodes domain knowledge, and introduce a domain-aware constraint to align the policy sampling distribution with this domain support during reinforcement learning. This constraint encourages domain-consistent behaviors such as invariance and symmetry. Second, we quantify the degree of domain knowledge exhibited by each sampled output by measuring the divergence between the policy distribution and the domain-support distribution, and use this signal to reweight reinforcement learning advantages. Together, these two mechanisms enable effective and stable injection of abstract domain knowledge into MLLMs.

3.1. Preliminary

GRPO (Shao et al., 2024) is a value-free policy optimization method designed to improve training stability and sample efficiency in reinforcement learning. Derived from Proximal Policy Optimization (PPO) (Schulman et al., 2017), GRPO avoids explicit value function estimation by adopting a group-based relative advantage formulation, which effectively regularizes policy updates while preserving sufficient optimization flexibility. Let π_θ denote a policy parameterized by θ . Given an input context c , GRPO first draws a group of G candidate outputs $\{o_1, o_2, \dots, o_G\}$ from the previous policy $\pi_{\theta_{\text{old}}}$. Each sampled output is then evaluated by predefined, verifiable reward functions, producing a set of scalar rewards $\{r_1, r_2, \dots, r_G\}$. Instead of relying on a learned value baseline, GRPO computes relative advantages within the sampled group by normalizing rewards as

$$A_i = \frac{r_i - \text{mean}(\{r_1, r_2, \dots, r_G\})}{\text{std}(\{r_1, r_2, \dots, r_G\})}. \quad (1)$$

Using the resulting group-relative advantages $\{A_1, A_2, \dots, A_G\}$, the policy π_θ is optimized by maximizing the following objective:

$$\mathcal{L}(\theta) = \mathbb{E}_{\{o_i\}_{i=1}^G \sim \pi_{\theta_{\text{old}}}} \left[\frac{1}{G} \sum_{i=1}^G \frac{\pi_\theta(o_i)}{\pi_{\theta_{\text{old}}}(o_i)} A_i - \beta \mathbb{D}_{\text{KL}}(\pi_\theta \parallel \pi_{\text{ref}}) \right], \quad (2)$$

where $\mathbb{D}_{\text{KL}}(\cdot \parallel \cdot)$ denotes the Kullback–Leibler divergence that constrains the updated policy π_θ to remain close to a reference policy π_{ref} , and β controls the strength of this regularization.

3.2. Domain-aware Constraints

We adopt Group Relative Policy Optimization (GRPO) as the base reinforcement learning framework and employ the reward functions proposed in Visual-RFT (Liu et al., 2025) to supervise policy optimization. Given multimodal inputs consisting of prompt questions and domain-specific images, the model produces a policy sampling distribution π_θ , while

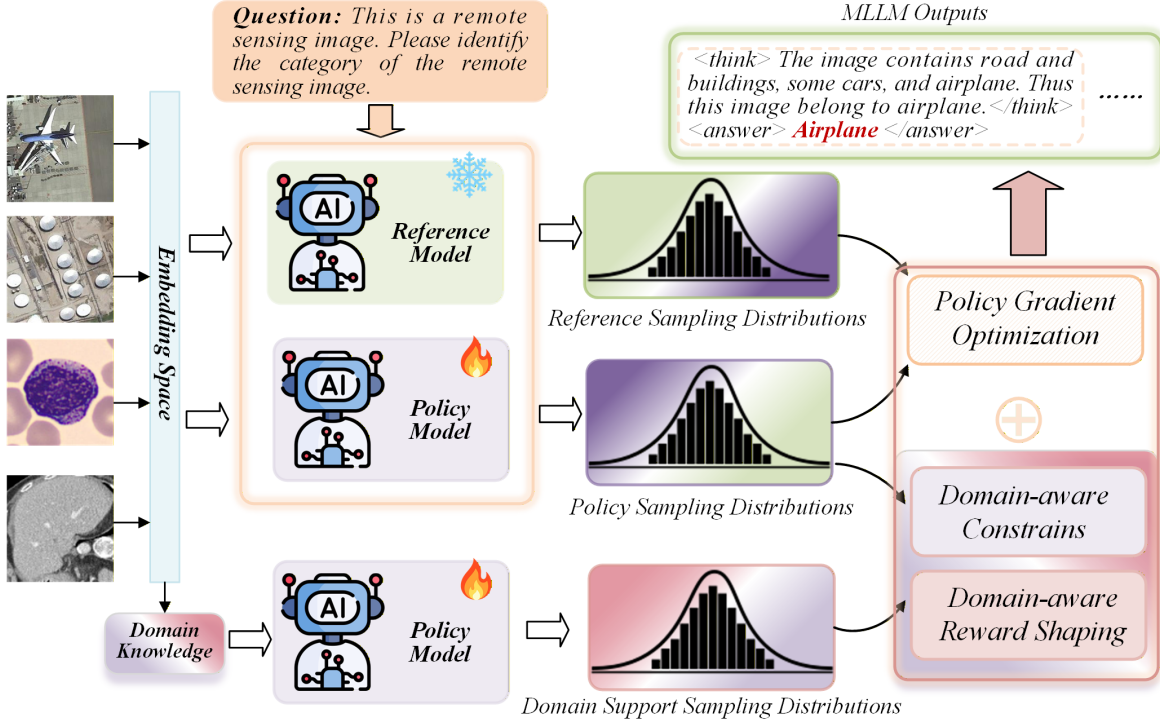


Figure 2. Overview of the proposed domain-aware reinforcement fine-tuning framework. Unlike prompt-based or caption-based domain adaptation, domain knowledge is incorporated at the optimization level through domain-aware constraints and reward shaping. By modifying the policy sampling distributions under reinforcement learning, the model is guided toward domain-consistent reasoning behaviors without relying on dense annotations.

a reference model provides a reference distribution π_{ref} . In GRPO, the Kullback–Leibler (KL) divergence between π_θ and π_{ref} is used to regularize policy updates, ensuring that the optimized policy remains close to the reference model and thus preserves general prior knowledge. Inspired by this mechanism, we further introduce a *domain-aware constraint* to explicitly inject domain knowledge into the policy optimization process.

Specifically, we consider rotation invariance in remote sensing and symmetry consistency in medical imaging as representative forms of domain knowledge. A straightforward approach would be to directly enforce invariance or consistency at the output or reward level. However, such explicit constraints are often brittle and task-dependent, and may fail to generalize across different prompts or output structures. Instead, we incorporate domain knowledge at the distribution level by regulating the policy sampling behavior under domain-specific transformations. To construct a domain-support sampling distribution, we apply domain-specific transformations, random rotations for remote sensing images and symmetric transformations for medical images, and feed the transformed inputs, together with the same prompt questions, into the policy model. This process yields a domain-support sampling distribution denoted as π_θ^D . To enforce invariance and consistency, we minimize the KL divergence between the original policy distribution π_θ and the

domain-support distribution π_θ^D , which defines the domain loss:

$$\mathcal{L}_{\text{dom}} = \mathbb{D}_{\text{KL}}(\pi_\theta^D \parallel \pi_\theta). \quad (3)$$

By constraining the policy sampling distribution to remain consistent under domain-specific transformations, this loss encourages the model to exhibit domain-invariant and domain-consistent behaviors.

3.3. Domain-aware Reward Shaping

Beyond domain-aware constraints, we further introduce *domain-aware reward shaping* to provide fine-grained optimization signals that explicitly emphasize domain-consistent behaviors. While the constraint term enforces distribution-level invariance globally, it treats all samples equally. In contrast, domain-aware reward shaping allows the optimization process to adaptively focus on samples that better satisfy domain principles.

Inspired by group-based relative evaluation in GRPO, we quantify the degree of domain knowledge exhibited by each sampled output by measuring the divergence between the policy sampling distribution π_θ and the domain-support distribution π_θ^D . We use KL divergence for constraints due to its asymmetry and stronger penalization of distributional mismatch, while JS divergence is adopted for advantage reweighting due to its boundedness and stability. Specifically,

we compute the Jensen–Shannon (JS) divergence as

$$\mathcal{D}_i = \mathbb{D}_{\text{JS}}(\pi_\theta^D \parallel \pi_\theta), \quad (4)$$

which yields a bounded and symmetric measure in $[0, 1]$ that reflects how well a sample aligns with the domain-support distribution. Using this divergence, we reweight the original GRPO advantages to obtain *domain-aware advantages*. Samples that are more consistent with domain knowledge (i.e., smaller divergence) are assigned larger advantages:

$$A_i^d = (1 - \mathcal{D}_i) \cdot A_i. \quad (5)$$

By incorporating the domain-aware advantages, the GRPO objective is modified as

$$\mathcal{L}(\theta) = \mathbb{E}_{\{o_i\}_{i=1}^G \sim \pi_{\theta_{\text{old}}}} \left[\frac{1}{G} \sum_{i=1}^G \frac{\pi_\theta(o_i)}{\pi_{\theta_{\text{old}}}(o_i)} A_i^d - \beta \mathbb{D}_{\text{KL}}(\pi_\theta \parallel \pi_{\text{ref}}) - \mathbb{D}_{\text{KL}}(\pi_\theta^D \parallel \pi_\theta) \right]. \quad (6)$$

More generally, the resulting *domain-aware reinforcement learning objective* can be written as

$$\mathcal{L}_{\text{DA}}(\theta) = \mathbb{E}_{\{o_i\}_{i=1}^G \sim \pi_{\theta_{\text{old}}}} \left[\frac{1}{G} \sum_{i=1}^G \frac{\pi_\theta(o_i)}{\pi_{\theta_{\text{old}}}(o_i)} A_i^d - \beta \mathbb{D}_{\text{KL}}(\pi_\theta \parallel \pi_{\text{ref}}) - \mathcal{L}_{\text{dom}} \right]. \quad (7)$$

Although we instantiate framework with rotation invariance and symmetry consistency, the proposed formulation is general and can incorporate arbitrary domain priors that can be expressed via transformations or distributional constraints.

4. Experiments

4.1. Experimental Setups

To evaluate our method under realistic specialized-domain scenarios, we conduct few-shot learning experiments in both remote sensing and medical imaging domains. For the remote sensing domain, we consider six widely used benchmark datasets: UCM (Yang & Newsam, 2010), AID (Xia et al., 2017), RSICD (Lu et al., 2017), WHURS19 (Dai & Yang, 2011), PatternNet (Zhou et al., 2018), and NWPU (Cheng et al., 2017). For the medical imaging domain, we adopt datasets from MedMNIST v2 (Yang et al., 2023), including OrganAMNIST, BloodMNIST, DermaMNIST, PathMNIST, and TissueMNIST.

We conducted experiments under 1-shot, 2-shot, 4-shot, and 8-shot settings, where the number of shots denotes the number of annotated samples per category. We adopt

Table 2. Few-shot results on the remote sensing domain. We conducted experiments on six remote sensing datasets. Δ denotes the performance benefits compared with SFT.

Models	Average	UCM	AID	RSICD	WHURS19	PatternNet	NWPU
Qwen2.5-VL	16.0	8.91	18.6	15.5	29.3	8.61	14.9
1-shot							
SFT	16.8	10.1	19.8	15.7	30.3	9.15	15.6
Visual-RFT	17.4	10.3	20.9	16.1	30.7	9.61	16.5
Ours	19.7	16.1	22.0	17.1	33.7	10.8	18.4
Δ	+2.9	+6.0	+2.2	+1.4	+3.4	+1.7	+2.8
2-shot							
SFT	18.3	14.9	20.6	16.0	31.2	10.4	16.6
Visual-RFT	19.1	15.7	21.8	16.2	31.7	11.9	17.2
Ours	20.9	17.1	23.8	19.6	33.6	12.6	18.7
Δ	+2.6	+2.2	+3.2	+3.6	+2.4	+1.2	+2.1
4-shot							
SFT	20.3	17.0	21.8	19.8	32.3	12.0	18.9
Visual-RFT	21.9	18.4	22.4	23.5	32.6	12.5	21.8
Ours	25.0	20.1	24.4	25.8	38.8	17.5	23.5
Δ	+4.7	+3.1	+2.6	+6.0	+6.5	+5.5	+4.6
8-shot							
SFT	25.5	21.8	29.9	22.6	39.5	15.4	23.6
Visual-RFT	28.5	23.6	32.9	25.6	40.2	18.2	30.5
Ours	32.3	28.8	38.9	26.4	44.4	19.1	36.4
Δ	+7.8	+7.0	+9.0	+3.8	+4.9	+3.7	+12.8

the reward functions in Visual-RFT (Liu et al., 2025) to reward the policy model. To further assess the effectiveness of our approach in multimodal reasoning, we additionally conduct few-shot grounding experiments on the DIOR (Li et al., 2020) dataset. All experiments are conducted using Qwen2.5-VL as the base MLLM. Training is performed with a batch size of 4 on 2 or 4 NVIDIA A100 GPUs (80GB). The model is trained for 2 epochs in the 1-shot and 2-shot settings, and for 4 epochs in the 4-shot and 8-shot settings. We use the Adam optimizer with a learning rate of 5×10^{-5} . Unless otherwise specified, all experiments use the same prompt templates and evaluation protocols.

4.2. Quantitative Results

Remote sensing domain. Table 2 reports the few-shot recognition results on six remote sensing datasets using Qwen2.5-VL-3B. Our method consistently outperforms both SFT and Visual-RFT across all shot settings and all datasets. Notably, the performance gains become more pronounced as the number of shots increases, indicating that domain-aware reinforcement fine-tuning can more effectively leverage limited supervision. On average, our approach improves over SFT by **+2.9**, **+2.6**, **+4.7**, and **+7.8** points under the 1-shot, 2-shot, 4-shot, and 8-shot settings, respectively. Substantial

Table 3. Few-shot results on the medical imaging domain. We conducted experiments on five medical imaging datasets. Δ denotes the performance benefits compared with SFT.

Models	Average	OrganAMNIST	BloodMNIST	DermaMNIST	PathMNIST	TissueMNIST
Qwen2.5-VL	20.7	8.70	14.8	21.7	29.0	29.1
1-shot						
SFT	20.9	9.10	15.2	21.3	29.8	29.5
Visual-RFT	21.0	9.39	15.2	21.1	29.9	29.5
Ours	21.5	9.85	15.6	21.8	30.6	29.7
Δ	+0.6	+0.75	+0.4	+0.5	+0.8	+0.2
2-shot						
SFT	21.4	9.76	15.5	21.8	30.1	29.8
Visual-RFT	21.6	9.81	15.6	22.3	30.3	29.8
Ours	23.2	12.4	16.1	23.5	33.2	30.9
Δ	+1.8	+2.6	+0.6	+1.7	+3.1	+1.1
4-shot						
SFT	22.9	10.0	16.1	27.3	30.6	30.3
Visual-RFT	23.0	10.1	16.0	27.6	30.9	30.6
Ours	25.3	13.2	17.2	32.8	31.4	31.7
Δ	+2.4	+3.2	+1.1	+5.5	+0.8	+1.4
8-shot						
SFT	24.1	10.7	17.1	28.9	32.3	31.4
Visual-RFT	24.4	10.8	17.4	29.9	32.6	31.5
Ours	26.8	13.3	18.9	33.1	35.4	33.1
Δ	+2.7	+2.5	+1.8	+4.2	+3.1	+1.7

improvements are observed on datasets that exhibit strong rotational characteristics, such as WHURS19, PatternNet, and NWPU, where our method achieves gains of up to **+6.5**, **+5.5**, and **+12.8** points. These results validate the effectiveness of injecting domain knowledge at the policy optimization level.

Medical imaging domain. Table 3 summarizes the few-shot recognition results on five medical imaging benchmarks using Qwen2.5-VL-3B. Compared with remote sensing, the improvements in the 1-shot setting are relatively modest, which is expected due to the higher visual homogeneity and label ambiguity in medical images. Nevertheless, our method consistently outperforms both SFT and Visual-RFT across all shot settings, achieving average gains over SFT of **+0.6**, **+1.8**, **+2.4**, and **+2.7** points from 1-shot to 8-shot. The advantages become more evident as the number of shots increases, particularly on datasets with strong anatomical symmetry such as OrganAMNIST and PathMNIST, where

Table 4. Few-shot grounding results on DIOR dataset of 6 representative categories. We conducted 4-shot and 8-shot experiments. Δ denotes the performance benefits compared with SFT. The first column denotes the average mAP.

Models	mAP	Airplane	Bridge	Harbor	Stadium	Storage Tank	Ship
Qwen2.5-VL	11.3	15.6	5.71	13.2	19.8	8.66	4.60
4-shot							
SFT	17.8	22.2	15.4	15.8	23.8	13.6	15.9
Visual-RFT	19.6	25.3	17.7	16.8	24.2	15.8	17.9
Ours	21.0	27.6	18.6	17.9	25.8	16.7	19.5
Δ	+3.2	+5.4	+3.2	+2.1	+2.0	+3.1	+3.6
8-shot							
SFT	22.1	27.1	17.9	26.7	25.1	16.9	18.7
Visual-RFT	22.7	27.3	18.8	27.9	25.9	17.1	19.2
Ours	24.6	29.9	20.6	29.6	27.8	18.4	21.3
Δ	+2.5	+2.8	+2.7	+2.9	+2.7	+2.5	+2.6

our method yields gains of up to **+3.2** and **+5.5** points. These results demonstrate that enforcing symmetry consistency at the distribution level effectively injects structural medical priors and improves few-shot generalization.

Few-shot grounding. Following the experimental protocol of Visual-RFT (Liu et al., 2025), we randomly sample six representative categories from the DIOR dataset and evaluate few-shot grounding performance using the larger Qwen2.5-VL-7B model, as reported in Table 4. Our method consistently outperforms both SFT and Visual-RFT under the 4-shot and 8-shot settings. In particular, it achieves average mAP improvements of **+3.2** and **+2.5** over SFT in the 4-shot and 8-shot scenarios, respectively. Performance gains are observed across all six object categories, including Airplane, Bridge, and Ship, demonstrating more accurate spatial localization and region-level reasoning. These results indicate that domain-aware reinforcement fine-tuning not only improves classification performance but also effectively enhances multimodal grounding capabilities when applied to larger-capacity models.

4.3. Qualitative Results

Figure 3 presents the qualitative comparisons between SFT and our method across both remote sensing and medical imaging domains. Particularly, the first row denotes samples in the remote sensing domain, while the second row denotes results in medical imaging domain. For remote sensing scenes, SFT often produces coarse or semantically incorrect predictions, such as confusing bridges with forests,



Figure 3. Qualitative results on remote sensing and medical imaging tasks. Compared with directly supervised fine-tuning (SFT), our method yields accurate and fine-grained categories by grounding predictions in discriminative visual patterns and domain-specific cues. First Row: Remote Sensing. Second Row: Medical Imaging.

parking lots with generic vehicle-related categories, or railway stations with urban areas. In contrast, our method correctly identifies fine-grained scene categories by grounding predictions in discriminative spatial structures and object arrangements, e.g., linear bridge spans over water, dense vehicle layouts in parking lots, and track-centered configurations in railway stations. Similar improvements are observed in the medical imaging domain. While SFT tends to generate superficial or noisy predictions (e.g., confusing debris with lymphocytes or misclassifying tissue types), our approach produces clinically meaningful categories such as colorectal adenocarcinoma, lymphocytes, and immature granulocytes. These predictions are supported by coherent visual reasoning that aligns cellular morphology with domain-specific semantics. Overall, the results demonstrate that domain-aware reinforcement fine-tuning effectively enhances cross-domain visual reasoning and semantic grounding. Our method not only improves answer correctness but also yields more interpretable and visually consistent predictions, highlighting its robustness in both complex remote sensing scenes and fine-grained medical imagery.

4.4. Ablation Study

Effect of domain-aware reinforcement learning components. Table 5 reports the ablation results of the proposed domain-aware reinforcement learning components on the UCM dataset under different few-shot settings. Starting from the baseline without any domain-aware design, in-

Table 5. Ablation study of domain-aware reinforcement learning components on the UCM dataset. DC denotes domain-aware constraint and DR denotes domain-aware reward shaping.

DC	DR	1-shot	2-shot	4-shot	8-shot
✗	✗	10.3	15.7	18.4	23.6
✓	✗	14.5	16.8	19.1	26.5
✗	✓	15.4	16.6	19.8	27.7
✓	✓	16.1	17.1	20.1	28.8

roducing either the domain-aware constraint (DC) or the domain-aware reward shaping (DR) consistently improves performance across all shot numbers, demonstrating that both components are individually effective. In particular, DC yields more pronounced gains in extremely low-shot settings, indicating its effectiveness in constraining the policy toward domain-consistent behaviors, while DR provides larger improvements in higher-shot regimes by delivering more informative and stable reward signals. When both DC and DR are jointly applied, the model achieves the best performance in all settings, with clear and consistent margins over using either component alone. These results validate the complementary nature of DC and DR, and confirm that their combination is crucial for fully exploiting domain knowledge in reinforcement fine-tuning.

Comparison with Direct Data Augmentation. Table 6 compares our method with standard data augmentation (DA) strategies applied during training on the UCM dataset. As

Table 6. Comparison with direct data augmentation on the UCM dataset. DA denotes standard data augmentation applied during training. VRFT denotes Visual-RFT (Liu et al., 2025).

Method	1-shot	2-shot	4-shot	8-shot
SFT	10.1	14.9	17.0	21.8
SFT + DA	10.2	14.8	17.1	21.6
VRFT	10.3	15.7	18.4	23.6
VRFT + DA	10.4	15.8	18.3	23.7
Ours	16.1	17.1	20.1	28.8

Table 7. Ablation study comparing output-level constraints and distribution-level constraints on the UCM dataset. OC denotes output-level constraint, DC denotes domain-aware constraint and DR denotes domain-aware reward shaping.

Method	1-shot	2-shot	4-shot	8-shot
Baseline	10.3	15.7	18.4	23.6
Baseline + OC	11.5	15.9	18.6	23.5
Baseline + DC	14.5	16.8	19.1	26.5
DC + DR (Ours)	16.1	17.1	20.1	28.8

shown, incorporating conventional data augmentation into either SFT or Visual-RFT leads to only marginal performance changes, and in some cases even results in slight degradation, particularly under low-shot settings. This suggests that naive data-level transformations are insufficient to effectively capture domain-specific invariances and may introduce additional noise when supervision is extremely limited. In contrast, our domain-aware reinforcement fine-tuning significantly outperforms all baselines by a large margin across all shot numbers. Notably, the performance gap becomes increasingly pronounced as the number of shots increases, highlighting that explicitly injecting domain knowledge at the policy optimization level is substantially more effective than relying on direct data augmentation. These results further confirm that domain-aware RL provides a more principled and robust mechanism for exploiting structural priors than conventional augmentation-based approaches.

Output-level vs. Distribution-level Constraints. Table 7 investigates the effectiveness of enforcing domain knowledge at different levels, comparing output-level constraints (OC) with distribution-level constraints incorporated into reinforcement learning. Applying output-level constraints on top of the baseline yields only marginal improvements, and the gains are inconsistent across shot settings, indicating limited capability in capturing domain-specific invariances. In contrast, introducing domain-aware constraints at the distribution level (DC) leads to substantially larger and more stable performance gains across all shot numbers, demonstrating that enforcing consistency over model behaviors is more effective than directly regularizing final predictions. Furthermore, combining distribution-level constraints with domain-aware reward shaping (DC + DR) achieves the best performance by a clear margin, highlighting the complementary roles of constraint-based regularization and reward-

Table 8. Effect of divergence choices for domain-aware constraint (DC) and domain-aware reward shaping (DR) on the UCM dataset. Div. denotes Divergence.

DC Div.	DR Div.	1-shot	2-shot	4-shot	8-shot
KL	KL	14.8	16.5	18.7	26.5
JS	JS	15.7	16.8	19.5	27.6
JS	KL	13.9	16.1	17.6	25.3
KL(Ours)	JS (Ours)	16.1	17.1	20.1	28.8

driven optimization. These results confirm that injecting domain knowledge at the policy and distribution level is crucial for robust few-shot generalization, while output-level heuristics alone are insufficient.

Divergence Choices for Varying Components. Table 8 analyzes the impact of different divergence functions used in domain-aware constraint (DC) and domain-aware reward shaping (DR). When the same divergence is applied to both components (KL–KL or JS–JS), performance improves over the baseline but remains suboptimal, suggesting that DC and DR play distinct roles and benefit from different divergence characteristics. Using JS divergence for DC provides more stable improvements than KL, as JS is symmetric and bounded, making it better suited for enforcing distribution-level consistency. Conversely, employing KL divergence for DR leads to inferior performance, indicating that asymmetric penalties in reward shaping may destabilize policy optimization. Our final design, which applies KL divergence for DC and JS divergence for DR, achieves the best results across all shot settings. This complementary combination effectively balances strict distribution alignment and stable reward optimization, highlighting the importance of carefully selecting divergence functions for different components in domain-aware reinforcement learning.

5. Conclusion

We propose a domain-aware reinforcement fine-tuning framework that injects abstract domain knowledge into multimodal large language models at the policy distribution level. By combining domain-aware constraints with domain-aware reward shaping, our method enforces domain-knowledge consistent behaviors directly during reinforcement learning. Extensive experiments across remote sensing and medical imaging benchmarks demonstrate consistent improvements under few-shot settings, and ablation studies confirm the complementary roles of the proposed components. These results suggest that domain-aware reinforcement learning is an effective and general approach for adapting multimodal foundation models to specialized domains with limited supervision. We believe this framework provides a promising direction for systematically integrating domain priors into multimodal models beyond the specific tasks studied in this work.

References

Achiam, J., Adler, S., Agarwal, S., Ahmad, L., Akkaya, I., Aleman, F. L., Almeida, D., Altenschmidt, J., Altman, S., Anadkat, S., et al. Gpt-4 technical report. *arXiv:2303.08774*, 2023.

Bai, S., Chen, K., Liu, X., Wang, J., Ge, W., Song, S., Dang, K., Wang, P., Wang, S., Tang, J., et al. Qwen2. 5-vl technical report. *arXiv:2502.13923*, 2025.

Cao, Q., Chen, Y., Lu, L., Sun, H., Zeng, Z., Yang, X., and Zhang, D. Generalized domain prompt learning for accessible scientific vision-language models. *Nexus*, 2(2), 2025.

Cheng, D., Huang, S., Zhu, Z., Zhang, X., Zhao, W. X., Luan, Z., Dai, B., and Zhang, Z. On domain-adaptive post-training for multimodal large language models. *arXiv:2411.19930*, 2024.

Cheng, D., Huang, S., Zhu, Z., Zhang, X., Zhao, W. X., Luan, Z., Dai, B., and Zhang, Z. On domain-adaptive post-training for multimodal large language models. In *Findings of the Association for Computational Linguistics: EMNLP 2025*, pp. 274–296, 2025.

Cheng, G., Han, J., and Lu, X. Remote sensing image scene classification: Benchmark and state of the art. *Proceedings of the IEEE*, 105(10):1865–1883, 2017.

Dai, D. and Yang, W. Satellite image classification via two-layer sparse coding with biased image representation. *IEEE Transactions on Geoscience and Remote Sensing*, 8(1):173–176, 2011.

Dong, G., Yuan, H., Lu, K., Li, C., Xue, M., Liu, D., Wang, W., Yuan, Z., Zhou, C., and Zhou, J. How abilities in large language models are affected by supervised fine-tuning data composition. In *Proceedings of the 62nd Annual Meeting of the Association for Computational Linguistics (Volume 1: Long Papers)*, pp. 177–198, 2024.

Fan, W.-C., Chen, Y.-C., Liu, M., Yuan, L., and Sigal, L. On pre-training of multimodal language models customized for chart understanding. *arXiv:2407.14506*, 2024.

Gao, Z., Chang, J., Zhan, W., Oertell, O., Swamy, G., Brantley, K., Joachims, T., Bagnell, D., Lee, J. D., and Sun, W. Rebel: Reinforcement learning via regressing relative rewards. *Advances in Neural Information Processing Systems*, 37:52354–52400, 2024.

Guo, D., Yang, D., Zhang, H., Song, J., Wang, P., Zhu, Q., Xu, R., Zhang, R., Ma, S., Bi, X., et al. Deepseek-r1 incentivizes reasoning in llms through reinforcement learning. *Nature*, 645(8081):633–638, 2025.

Han, S. C., Cao, F., Poon, J., and Navigli, R. Multimodal large language models and tunings: Vision, language, sensors, audio, and beyond. In *Proceedings of the 32nd ACM International Conference on Multimedia*, pp. 11294–11295, 2024.

Huang, D., Yan, C., Li, Q., and Peng, X. From large language models to large multimodal models: A literature review. *Applied Sciences*, 14(12):5068, 2024a.

Huang, Y., Xie, L., Wang, X., Yuan, Z., Cun, X., Ge, Y., Zhou, J., Dong, C., Huang, R., Zhang, R., et al. Smartedit: Exploring complex instruction-based image editing with multimodal large language models. In *Proceedings of the IEEE/CVF Conference on Computer Vision and Pattern Recognition*, pp. 8362–8371, 2024b.

Jaech, A., Kalai, A., Lerer, A., Richardson, A., El-Kishky, A., Low, A., Helyar, A., Madry, A., Beutel, A., Carney, A., et al. Openai o1 system card. *arXiv:2412.16720*, 2024.

Jiang, J., Ma, C., Song, X., Zhang, H., and Luo, J. Corvid: Improving multimodal large language models towards chain-of-thought reasoning. In *Proceedings of the IEEE/CVF International Conference on Computer Vision*, pp. 3034–3046, 2025a.

Jiang, J.-P., Xia, Y., Sun, H.-L., Lu, S., Chen, Q.-G., Luo, W., Zhang, K., Zhan, D.-C., and Ye, H.-J. Multimodal tabular reasoning with privileged structured information. *arXiv:2506.04088*, 2025b.

Li, B., Ge, Y., Ge, Y., Wang, G., Wang, R., Zhang, R., and Shan, Y. Seed-bench: Benchmarking multimodal large language models. In *Proceedings of the IEEE/CVF Conference on Computer Vision and Pattern Recognition*, pp. 13299–13308, 2024.

Li, J., Li, D., Savarese, S., and Hoi, S. Blip-2: Bootstrapping language-image pre-training with frozen image encoders and large language models. In *International conference on machine learning*, pp. 19730–19742. PMLR, 2023.

Li, K., Wan, G., Cheng, G., Meng, L., and Han, J. Object detection in optical remote sensing images: A survey and a new benchmark. *ISPRS journal of photogrammetry and remote sensing*, 159:296–307, 2020.

Lin, J., Yin, H., Ping, W., Molchanov, P., Shoeybi, M., and Han, S. Vila: On pre-training for visual language models. In *Proceedings of the IEEE/CVF conference on computer vision and pattern recognition*, pp. 26689–26699, 2024.

Liu, A., Feng, B., Xue, B., Wang, B., Wu, B., Lu, C., Zhao, C., Deng, C., Zhang, C., Ruan, C., et al. Deepseek-v3 technical report. *arXiv:2412.19437*, 2024.

Liu, Z., Sun, Z., Zang, Y., Dong, X., Cao, Y., Duan, H., Lin, D., and Wang, J. Visual-rft: Visual reinforcement fine-tuning. In *Proceedings of the IEEE/CVF International Conference on Computer Vision (ICCV)*, pp. 2034–2044, October 2025.

Lu, S., Li, Y., Xia, Y., Hu, Y., Zhao, S., Ma, Y., Wei, Z., Li, Y., Duan, L., Zhao, J., et al. Ovis2. 5 technical report. *arXiv:2508.11737*, 2025.

Lu, X., Wang, B., Zheng, X., and Li, X. Exploring models and data for remote sensing image caption generation. *IEEE Transactions on Geoscience and Remote Sensing*, 56(4):2183–2195, 2017.

Luo, G., Yang, X., Dou, W., Wang, Z., Liu, J., Dai, J., Qiao, Y., and Zhu, X. Mono-internvl: Pushing the boundaries of monolithic multimodal large language models with endogenous visual pre-training. In *Proceedings of the Computer Vision and Pattern Recognition Conference*, pp. 24960–24971, 2025a.

Luo, R., Zhang, H., Chen, L., Lin, T.-E., Liu, X., Wu, Y., Yang, M., Li, Y., Wang, M., Zeng, P., et al. Mmevol: Empowering multimodal large language models with evol-instruct. In *Findings of the Association for Computational Linguistics: ACL 2025*, pp. 19655–19682, 2025b.

Rafailov, R., Sharma, A., Mitchell, E., Manning, C. D., Ermon, S., and Finn, C. Direct preference optimization: Your language model is secretly a reward model. *Advances in neural information processing systems*, 36: 53728–53741, 2023.

Ramesh, S. S., Hu, Y., Chaimalas, I., Mehta, V., Sessa, P. G., Bou Ammar, H., and Bogunovic, I. Group robust preference optimization in reward-free rlhf. *Advances in Neural Information Processing Systems*, 37:37100–37137, 2024.

Schulman, J., Wolski, F., Dhariwal, P., Radford, A., and Klimov, O. Proximal policy optimization algorithms. *arXiv:1707.06347*, 2017.

Shao, Z., Wang, P., Zhu, Q., Xu, R., Song, J., Bi, X., Zhang, H., Zhang, M., Li, Y., Wu, Y., et al. Deepseekmath: Pushing the limits of mathematical reasoning in open language models. *arXiv:2402.03300*, 2024.

Sun, H.-L., Zhou, D.-W., Li, Y., Lu, S., Yi, C., Chen, Q.-G., Xu, Z., Luo, W., Zhang, K., Zhan, D.-C., et al. Parrot: Multilingual visual instruction tuning. In *Forty-second International Conference on Machine Learning*, 2025.

Wang, C., Wang, Z., Xu, X., Tang, Y., Zhou, J., and Lu, J. Q-vlm: Post-training quantization for large vision-language models. *Advances in Neural Information Processing Systems*, 37:114553–114573, 2024a.

Wang, W., Ding, L., Zeng, M., Zhou, X., Shen, L., Luo, Y., Yu, W., and Tao, D. Divide, conquer and combine: A training-free framework for high-resolution image perception in multimodal large language models. In *Proceedings of the AAAI Conference on Artificial Intelligence*, volume 39, pp. 7907–7915, 2025a.

Wang, Y., Sun, Z., Zhang, J., Xian, Z., Biyik, E., Held, D., and Erickson, Z. Rl-vlm-f: Reinforcement learning from vision language foundation model feedback. *arXiv:2402.03681*, 2024b.

Wang, Y., Sun, H.-L., Huzhang, G., Chen, Q.-G., Xu, Z., Luo, W., Zhang, K., and Zhang, L. Triplets better than pairs: Towards stable and effective self-play fine-tuning for llms. In *The Thirty-ninth Annual Conference on Neural Information Processing Systems*, 2025b.

Xia, G.-S., Hu, J., Hu, F., Shi, B., Bai, X., Zhong, Y., Zhang, L., and Lu, X. Aid: A benchmark data set for performance evaluation of aerial scene classification. *IEEE Transactions on Geoscience and Remote Sensing*, 55:3965–3981, 2017.

Xu, W., Zhou, Y., Zhou, Y., Cao, Q., Li, S., Bu, J., Liu, B., Chen, Y., He, X., Zhao, X., et al. Probing scientific general intelligence of llms with scientist-aligned workflows. *arXiv:2512.16969*, 2025.

Yang, J., Shi, R., Wei, D., Liu, Z., Zhao, L., Ke, B., Pfister, H., and Ni, B. Medmnist v2-a large-scale lightweight benchmark for 2d and 3d biomedical image classification. *Scientific Data*, 10(1):41, 2023.

Yang, Y. and Newsam, S. Bag-of-visual-words and spatial extensions for land-use classification. In *Proceedings of the 18th SIGSPATIAL international conference on advances in geographic information systems*, 2010.

Yuan, H., Chen, Z., Ji, K., and Gu, Q. Self-play fine-tuning of diffusion models for text-to-image generation. *Advances in Neural Information Processing Systems*, 37: 73366–73398, 2024.

Yue, Y., Chen, Z., Lu, R., Zhao, A., Wang, Z., Song, S., and Huang, G. Does reinforcement learning really incentivize reasoning capacity in llms beyond the base model? *arXiv:2504.13837*, 2025.

Zang, Y., Li, W., Han, J., Zhou, K., and Loy, C. C. Contextual object detection with multimodal large language models. *International Journal of Computer Vision*, 133(2):825–843, 2025.

Zhang, J., Huang, J., Yao, H., Liu, S., Zhang, X., Lu, S., and Tao, D. R1-vl: Learning to reason with multimodal large language models via step-wise group relative policy optimization. *arXiv:2503.12937*, 2025a.

Zhang, J., Zhang, C., Lu, J., and Zhao, Y. Domain-specific large language models for fault diagnosis of heating, ventilation, and air conditioning systems by labeled-data-supervised fine-tuning. *Applied Energy*, 377:124378, 2025b.

Zhang, X., Sun, H., Zhang, Y., Feng, K., Lu, C., Yang, C., and Meng, H. Critique-grpo: Advancing llm reasoning with natural language and numerical feedback. *arXiv:2506.03106*, 2025c.

Zhang, Y., Tzeng, E., Du, Y., and Kislyuk, D. Large-scale reinforcement learning for diffusion models. In *European Conference on Computer Vision*, pp. 1–17. Springer, 2024.

Zhou, W., Newsam, S., Li, C., and Shao, Z. Patternnet: A benchmark dataset for performance evaluation of remote sensing image retrieval. *ISPRS journal of photogrammetry and remote sensing*, 145:197–209, 2018.